DOI: 10.1002/adsc.201700585

Advanced Synthesis & Catalysis

Mutagenesis-Independent Stabilization of Class B Flavin Monooxygenases in Operation

Leticia C. P. Goncalves,[a] Daniel Kracher,[b] Sofia Milker,[a] Michael J. Fink,[a,c,*] Florian Rudroff,[a,*] Roland Ludwig,[b,*] Andreas S. Bommarius,[d] and Marko D. Mihovilovic[a]

[a] Institute of Applied Synthetic Chemistry, Vienna University of Technology, Getreidemarkt 9/163, 1060 Vienna, Austria
Fax: (+43)-1-58801-16399; phone: (+43)-664-6058-87137; e-mail: florian.rudroff@tuwien.ac.at
[b] Biocatalysis and Biosensing Research Group, Department of Food Science and Technology, BOKU-University of Natural Resources and Life Sciences, Muthgasse 18, 1190 Vienna, Austria
Fax: (+43)-1-47654-75039; phone: (+43)-1-47654-75216; e-mail: roland.ludwig@boku.ac.at
[c] Department of Chemistry and Chemical Biology, Harvard University, 12 Oxford St, Cambridge, MA 02138, USA
E-mail: mfink@gmwgroup.harvard.edu
[d] School of Chemical and Biomolecular Engineering, School of Chemistry and Biochemistry, Georgia Institute of Technology, Atlanta, GA 30332, USA

Received: May 7, 2017; Published online: May 19, 2017

Supporting information for this article can be found under https://dx.doi.org/10.1002/adsc.201700585.

Abstract: This paper describes the stabilization of flavin-dependent monooxygenases under reaction conditions, using an engineered formulation of additives (the natural cofactors NADPH and FAD, and superoxide dismutase and catalase as catalytic antioxidants). This way, a 10^3- to 10^4-fold increase of the half-life was reached without resource-intensive directed evolution or structure-dependent protein engineering methods. The stabilized enzymes are highly valued for their synthetic potential in biotechnology and medicinal chemistry (enantioselective sulfur, nitrogen and Baeyer–Villiger oxidations; oxidative human metabolism), but widespread application was so far hindered by their notorious fragility. Our technology immediately enables their use, does not require structural knowledge of the biocatalyst, and creates a strong basis for the targeted development of improved variants by mutagenesis.

Keywords: biocatalysis; cofactors; enzyme stabilization; oxygenation; reactive oxygen species

Introduction

Flavin monooxygenases (FMOs) are ubiquitously involved in oxidative biological processes,[1] from microorganisms to humans,[2] with a diverse portfolio of reactions (C–H hydroxylations, heteroatom oxidations, epoxidations, Baeyer–Villiger oxidations, etc.) and an unusually broad substrate scope. They catalyze these difficult transformations with excellent selectivity, creating a wealth of biotechnological opportunities[3] and possibilities to study oxidative metabolism of drug molecules *in vitro*.[2a] FMOs depend on flavin and nicotinamide cofactors, and orchestrate the complex reaction[4] of these two electron-transferring agents with the primary substrate and molecular oxygen as the co-substrate in a highly dynamic protein scaffold,[5] nonetheless with tight control on selectivity. FMO subclasses A and B achieve this within a single polypeptide unit;[3,6] they are thus most interesting for synthetic purposes. Structural information from class B FMOs together with their cofactors is scarce (22 structures from five enzymes, see the Supporting Information, Table S1), and the importance of the cofactors to maintain enzyme stability and structure was mostly neglected, so far.[7]

A prominent member of class B, cyclohexanone monooxygenase from A*cinetobacter calcoaceticus* NCIMB 9871 (CHMO),[8] was recently engineered by directed evolution to produce esomeprazole, the active pharmaceutical ingredient (API) of the proton-pump inhibitor Nexium, on a multi dozen-gram scale.[9] A powerful demonstration of CHMO's potential, yet multiple rounds of mutagenesis (41 mutations) were required to increase stability and other parameters to an economically viable level. It is so far the only known industrial process from this class of

enzymes, but conceptual application studies abound in the literature,[10] for example, synthesis of API intermediates,[11] metabolites,[12] aroma compounds,[13] polyester monomers,[14] or platform chemicals.[15]

Despite the lack of knowledge about the origins of the poor stability, most other studies on stabilization chose to alter the protein structure – randomly,[21] or by design.[19,20] Their impact on the applicability of class B FMOs has been low, because absolute quantitative data of improvement are inconclusive: (i) operational (kinetic) stability, if at all determined, was so far only improved within an order of magnitude;[19–21] (ii) the effect of unspecific additives provided only a 1.3-fold increase of the half-life ($t_{1/2}$);[17] (iii) the stabilizing effect of NADPH, described in a single instance on 4-hydroxyacetophenone monooxygenase,[22] was never quantified; (iv) published values of CHMO's $t_{1/2}$ span approx. three orders of magnitude (wild-type only, Figure 1).[9,16–21] The impact of a most recently discovered thermostable CHMO[23] cannot be assessed yet, because its substrate profile is so far unknown.

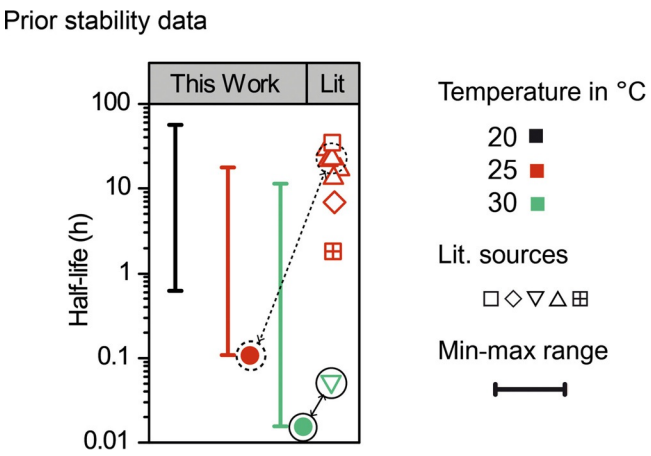

Figure 1. Functional stabilization of cyclohexanone monooxygenase from *Acinetobacter* sp. NCIMB 9871. Stability data (half-lives) from previous reports on this enzyme scatter over three orders of magnitude and show poor reproducibility; □ ref.[16], △ ref.[17], ◇ ref.[18], ▽ ref.[19], ⊞ ref.[20]. The two pairs of circled data points indicate identical enzyme incubation conditions (solid line) and comparable incubation conditions (dashed line).

We chose CHMO as our primary example for the engineering of a stabilizing formulation for class B FMOs, based on our analysis of: (i) the generic reaction mechanism, (ii) the cofactor binding, and (iii) the inevitable generation of reactive oxygen species (ROS). We evaluated stability in application-oriented metrics [total turnover number (TTN) and $t_{1/2}$] and under reaction conditions (kinetic stability), as opposed to equilibrium stability values (e.g., melting temperature T_m). These two different types of stabilities will often be causally linked, although quantitative expression requires knowledge of the deactivation kinetics,[24] rendering comparisons of their values virtually impossible.[25] Here, in addition to our engineered solution, we offer an experimentally backed hypothesis to correlate T_m and $t_{1/2}$, enabling further biochemical research.

Results and Discussion

First, we needed to identify the origins for the large variation in published stability data (Figure 1). We re-investigated the commonly used activity assay for NADPH-dependent FMOs and established reliable and reproducible conditions. Importantly, this relay assay (based on the absorbance of NADPH at 340 nm) can only quantify the total rate of oxygen activation, and not specifically any of the subsequent reaction pathways, which the formed peroxy intermediate can undergo. We found that *uncoupling* (the synthetically undesired decay of that intermediate to H_2O_2 or superoxide)[26] was often non-negligible to even dominant. This widely used assay is thus prone to producing misleading results, if not controlled diligently.

Ever since the initial kinetic characterization of CHMO using stopped-flow technique,[8a] most studies employed cuvette assays. By comparing slow (manual stirring) and fast (stopped-flow) mixing techniques, we found that manual mixing alone became a significant error source at short $t_{1/2}$ (seconds to minutes) in previous work. We thus chose either method based on the expected or observed time domain. Reproducible and rational control over the parameters of measurement provided the basis for investigations of the molecular components of the assay

NADPH Enhances Stability, but not $NADP^+$

We investigated the influence of the coenzyme (Table 1) and found CHMO to be highly unstable when incubated in buffered solution only ($t_{1/2} = 1.15$ min). Addition of the coenzyme in its oxidized form ($NADP^+$) or the substrate cyclohexanone did not change that value significantly (entries 2 and 3). We could exclude synergistic effects on stability of the two additives (entry 4) and furthermore could reproduce a recently published value for $t_{1/2}$, at least within the order of magnitude (the lowest published value; entries 4 *vs.* 5). Conversely, we observed a $t_{1/2}$ of approx. 2 h when the biocatalyst was incubated with the reduced coenzyme NADPH (entry 6) under otherwise identical conditions.

To understand the deactivation mechanism, we had to separate specific factors (structure stabilization)

Table 1. Comparison of $t_{1/2}$ values for CHMO using the oxidized and reduced coenzyme ($NADP^+$, NADPH) and the substrate cyclohexanone as additives at 30 °C. Residual activity of CHMO was assayed based on the commonly used relay quantification of cyclohexanone oxidation *via* decrease of NADPH absorbance, measured at 340 nm using purified enzyme; for details see the Supporting Information, Figure S1.

Entry	Incubation conditions before assay		Half-life [min]
1	0.1 μM CHMO		1.15 ± 0.03
2	0.1 μM CHMO	+ 0.2 mM $NADP^+$	1.17 ± 0.09
3	0.1 μM CHMO	+ 1.0 mM cyclohexanone	1.04 ± 0.07
4	0.1 μM CHMO PTDH fusion	+ 0.2 mM $NADP^+$ + 1.0 mM cyclohexanone	0.93 ± 0.05
5[19]	0.05 μM CHMO PTDH fusion	+ 0.1 mM $NADP^+$ + 0.5 mM cyclohexanone	3.17 ± 0.18
6	**0.1 μM CHMO**	**+ 0.2 mM NADPH**	**118 ± 29**

from unspecific (e.g., oxidative) deactivation, and therefore revisited the known secondary activity of FMOs. They also act as NADPH oxidases, thus producing H_2O_2, superoxide and $NADP^+$ from molecular oxygen and NADPH in an uncoupling reaction.[26,27] We measured rates of NADPH depletion using various additives and rates of H_2O_2 formation *via* a colorimetric assay, always starting from 100 μM NADPH (we determined K_M as approx. 4 μM at 25 °C; Lit.:[19,28] 6–16 μM).

Competitive substrate experiments using a fast converted substrate (cyclohexanone), a slowly converted substrate (4-phenylcyclohexanone), and none at all (uncoupling only) showed that the consumption rate of NADPH by CHMO in the absence of a substrate is high (and of second or higher order; Supporting Information, Figure S2 and Table S3). In these experiments we found little difference in the rates of H_2O_2 formation with the slow substrate and NADPH alone ($k_{uncoupling} = 2.5\ min^{-1}$ *vs.* $3.7\ min^{-1}$), but effective suppression of the undesired uncoupling reaction when the fast substrate cyclohexanone was used ($k_{uncoupling} = 1.1 \times 10^{-2}\ min^{-1}$). These results established that the enzyme deactivation rate was greatly reduced, as long as NADPH was present, and that the rate of unproductive oxidation was dependent on the rate of the primary oxidation reaction. Enzyme stability thus increased with a fast synthetic reaction, *and* larger available amounts of NADPH.

This effect did not scale linearly: whereas repeated, regular addition of the same amount of NADPH (replenishing to 100 μM) gave consistent results, a single addition to 2.5 mM for an overnight experiment gave unexpectedly high stability values.

To explain the effect of the concentration, we measured the equilibrium stability of CHMO at various concentrations of NADPH using differential scanning fluorimetry (DSF) of the intrinsic tryptophan fluorescence signal (CHMO contains 12 tryptophan residues, or 2.2% of amino acids). We recorded unfolding curves from 0.25–2.50 mM NADPH, and found a steep jump of the transition midpoint temperature (T_m) from the commonly reported value[19] of 38 °C to 50 °C at approx. 1 mM NADPH (Figure 2).

We then performed our standard activity assay at two temperatures (well above and below the two T_m values) and at two concentration levels of NADPH (well above and below the jump interval). Consistent with the results from DSF, we observed much higher kinetic stability using more NADPH at equal temperature (Figure 2).[29] These results clearly and quantitatively connected thermodynamic and kinetic stability of CHMO *via* the concentration of NADPH. In all cases, only the reduced cofactor had a measurable stabilizing effect on CHMO.

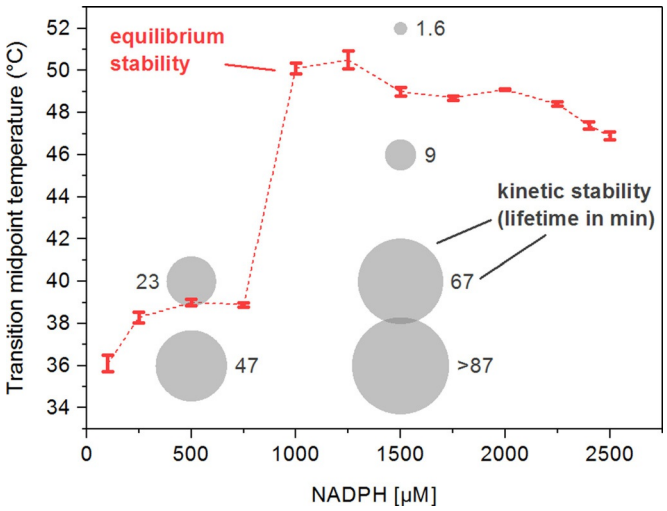

Figure 2. Equilibrium and kinetic stability of CHMO are significantly enhanced above 1 mM NADPH. Transition midpoint temperatures (or melting temperature, T_m) of 15 μM CHMO were determined using nDSF at various concentrations of NADPH (orange curve; reported as mean ± 1 SD, n = 3); kinetic stability values (as total average lifetime = $t_{plateau} + t_{1/2}/\ln 2$, see the Supporting Information) were obtained from the exponential fit of the stability curves (using 1 μM CHMO and 100 μM FAD) at selected temperature-NADPH pairs (Supporting Information, Figure S3); kinetic data is reported as mean values (n = 3), error data are given in the Supporting Information, Table S4.

FAD Readily Dissociates from Class B FMOs

CHMO is monomeric in solution, and binds to FAD non-covalently with 1:1 stoichiometry. We used two methods to determine the dissociation constant K_d for FAD: (i) a direct measurement of the binding to FAD using a fluorescence assay,[30] and (ii) an indirect estimation for K_d *via* determination of the FAD-dependent specific activity.[31] Both required apo-CHMO, which we obtained according to a published protocol,[32] and were performed immediately after de-flavination.

In the first method, we recorded the quenching of fluorescence of free FAD upon titration of 1 μM FAD with apo-CHMO (0.8–9.0 μM); we determined a K_d of 4.0 ± 0.4 μM. For the second method, we incubated the apoenzyme with various amounts of FAD (0–200 μM) for 5 min, and then measured the activity of the (partially) reconstituted enzyme in cuvettes. Logistic fitting of the data gave an estimate for K_d of 3.5 ± 0.6 μM (Supporting Information, Figure S4). The two values were statistically indistinguishable ($p < 0.001$), and indicated a strong dependence of CHMO's activity on the concentration of FAD. We thus examined the $t_{1/2}$ using combinations of various enzyme concentrations (0.1, 1, 10 and 100 μM) and defined ratios/concentrations of exogenous FAD (0, 10 and 100 μM FAD; Figure 3). An increase in cofactor concentration also stabilized the biocatalyst activity with approx. linear dependency: $t_{1/2}$ was augmented 1.5-fold by a 10-fold increase of exogenous FAD over the tested interval.

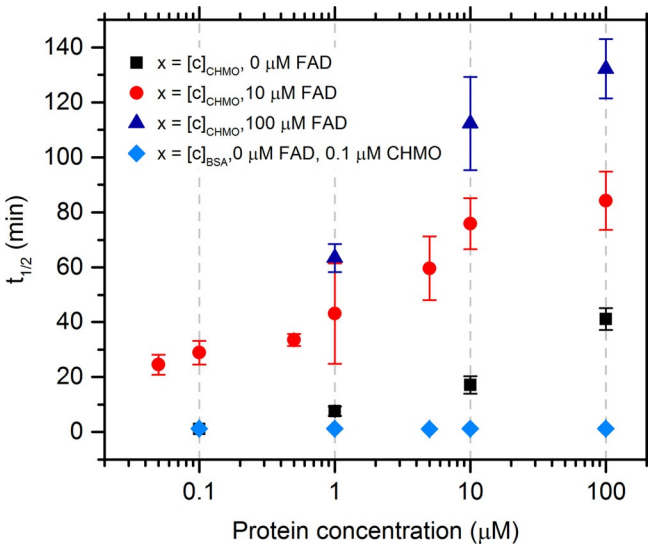

Figure 3. The activity and stability of CHMO is strongly enhanced by excess availability of the FAD cofactor (exogenous and dissociated FAD, the latter is dependent on the protein concentration).[32] Effect of specific protein-protein interactions, of various concentrations of FAD and BSA (Supporting Information, Tables S5 and S6) and the concentration of CHMO itself on the stability at 30 °C; measurements in cuvettes except: 0.1 μM CHMO without FAD (stopped-flow); see also Supporting Information, Tables S5 and S6 (deactivation rate constants) and Supporting Information, Figures S6 and S7 (kinetic curves). Data are reported as mean ± 1 SD (n = 3).

In summary for this section, we identified conditions that increase the $t_{1/2}$ from approx. 1 min (0.05 μM CHMO) to more than 2 h (100 μM CHMO with 100 μM FAD), utilizing the synergistic effects of high cofactor and biocatalyst concentration. This improvement was independent of the NADPH-mediated stabilization.

In vivo ROS Protection can be used *in vitro*

We had already scrutinized the influence of uncoupling on stability from the substrate side (accelerated decay of CHMO after depletion of NADPH), but any detrimental contribution of its products H_2O_2 and superoxide remained to be assessed. To counteract potential damage from ROS we used the redox-neutral catalysts superoxide dismutase (SOD) and catalase (CAT).

We found that the addition of SOD and CAT had a measurable, but small, positive effect on the $t_{1/2}$ of CHMO when no other additive (Figure 4a, Conditions a *vs.* b) or only FAD (Conditions c *vs.* d) was added to the buffer. When NADPH was added, the detrimental effects of the products from the uncoupling reactions were observed. Addition of SOD (400 U mL^{-1}) led to a reduction of $t_{1/2}$ by approx. 50% (Conditions e *vs.* f), whereas we did not observe any significant change using only CAT (Conditions e *vs.* g). To explain this finding in detail, we analyzed the effect of SOD on the H_2O_2 concentration. We found that SOD almost doubled the final titer of H_2O_2, when a poor substrate, or none at all was present. We could not measure any significant difference in the presence of the good substrate cyclohexanone (Supporting Information, Figure S8).

On the contrary, the combination of both enzymes increased $t_{1/2}$ approx. 1.5-fold under otherwise identical conditions (Conditions e *vs.* h). This effect was even greater at a higher concentration of NADPH (2.5 mM): the kinetic stability of CHMO was improved 4–8-fold (Conditions i *vs.* k). We also performed this experiment without FAD to deconvolute the individual contributions to the enhancement of stability. At this level, the observed difference was insignificant (Conditions j *vs.* k). Concluding from all our previous tests we eventually performed an experiment using the optimum set of additives (high FAD and NADPH loading, CAT and SOD addition) to gauge the synergism of all additives. We reproducibly found a $t_{1/2}$ of approx. 11 h (±7%) at 30 °C (Condi-

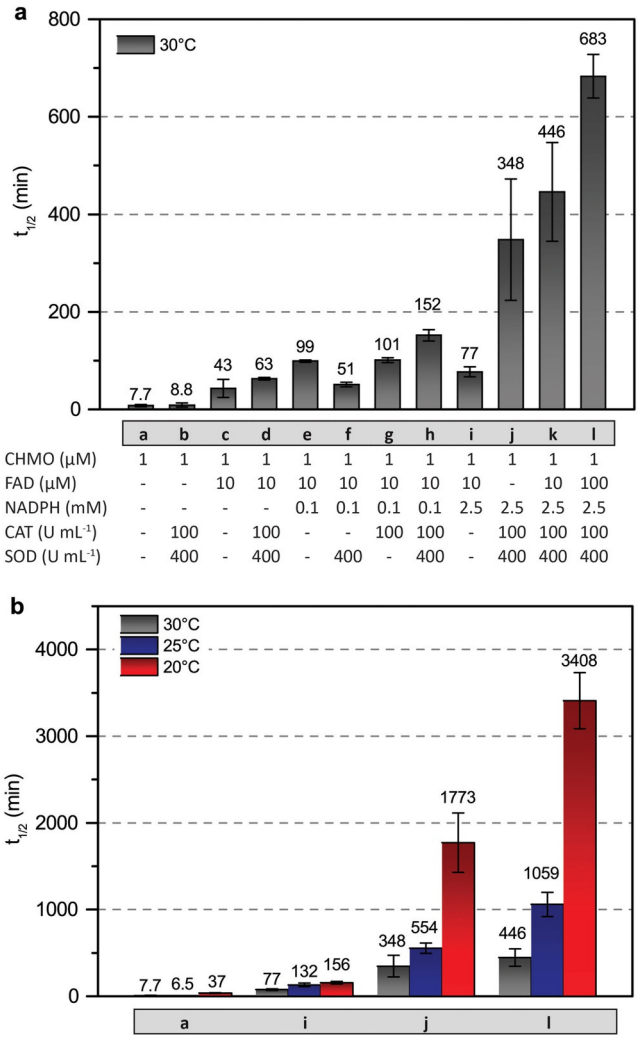

Figure 4. NADPH, FAD and ROS-degrading enzymes strongly stabilize FMOs, with highest effect at 20 °C. SOD and CAT were added in large excess over CHMO activity, but their ratio not necessarily prevented the accumulation of superoxide (see the Supporting Information, Methods). All $t_{1/2}$ values including these enzymes are thus to be interpreted as the lower limits. (a) $t_{1/2}$ of CHMO at 30 °C in the presence of stabilizing additives. (b) $t_{1/2}$ of CHMO at different temperatures in the presence of stabilizing additives; see the Supporting Information, Table S7 (deactivation rate constants) and Figures S9–S11 (kinetics curves). Data are reported as mean ±1 SD (n = 3).

tions l), which translates to an 88-fold improvement over 1 μM CHMO (Conditions a *vs.* l), and approx. 600-fold over 0.1 μM CHMO without additives (Table 1, entry 1).

Over the course of our studies we became aware of the critical role of temperature on CHMO stability. We initially chose 30 °C as the standard assay temperature for reasons of comparability with recently published values, but observed high variation in stability whenever the temperature was not accurately controlled. We therefore incubated CHMO at exactly 20, 25 and 30 °C in combination with three sets of additives to quantify the influence of temperature on the kinetic stability (Figure 4b). Without additives CHMO has a five-fold longer $t_{1/2}$ at 20 °C compared to 30 °C (Conditions a). Upon addition of NADPH and FAD (Conditions b) we found a strong increase in kinetic stability at all temperatures, but the difference between 20 and 30 °C was reduced to a factor of two. When we added SOD and CAT to counteract the uncoupling reaction the $t_{1/2}$ increased tremendously. When incubating CHMO at 20 °C with all additives, we measured a $t_{1/2}$ of approx. 57 h (±10%) which corresponds to a 92-fold improvement over solely CHMO in buffer at equal temperature, or approx. 3000-fold to the initial conditions without additives at 30 °C (Table 1, entry 1).

Other FMOs are Equally Stabilized by Additives

We chose two other enzymes to test our hypothesis that the identified origins of deactivation were common to class B FMOs: (i) a distantly related *Pseudomonad* class B FMO (OTEMO), which is also dependent on FAD and NADPH. Its $t_{1/2}$ was previously reported with 9 min at 30 °C, without specified additives.[33] We could reproduce this value under comparable conditions (Supporting Information, Table S8). (ii) A rhodococcal FMO (FMO-E),[34] representing a peculiar subgroup of class B FMOs: it accepts both NADH and NADPH, and was chosen as a second candidate because of its known structural divergence. It was still compatible with our assay (FMO-E was reported to catalyze Baeyer–Villiger oxidations). There was no prior published record of stability data for this biocatalyst.

We de-flavinated both enzymes and reconstituted the apoenzymes to determine the affinity for FAD, using the same protocol as described for CHMO. We were able to determine a slightly higher affinity towards the cofactor for OTEMO ($K_d = 0.94 \pm 0.16$ μM). FMO-E was too unstable in its apo form to allow the measurement of the dissociation constant; its $t_{1/2}$ without additives was much shorter than 2 min. We then chose two sets of additive combinations to test the generic applicability of our concept: both included SOD and CAT, but varied in FAD (10 and 100 μM) and NADPH (0.1 and 2.5 mM) concentrations (Supporting Information, Table S8, entries 2 and 3). In both series of experiments, we measured a large and significant improvement of kinetic stability for both enzymes. At high concentrations, we found a similar mean relative increase of $t_{1/2}$ for all three FMOs (CHMO: 90-fold, OTEMO: 49-fold, FMO-E: at least 78-fold, Supporting Information, Table S8, entry 3).

The Gain in $t_{1/2}$ is Fully Retained under Turnover Conditions

As a verification of applicability, we wanted to transfer the improvement of kinetic stability to a running reaction set-up. We chose 4-phenylcyclohexanone as a model substrate: it is prochiral, reportedly converted at a low rate,[35] and it is not volatile. The first property enabled the demonstration in an asymmetric transformation, arguably a major feature of CHMO. The other, technical properties allowed the measurement of kinetic stability over more than one period of $t_{1/2}$, while there was still substrate available. Also, as shown earlier, the slow reaction rate would promote uncoupling, therefore allowing us to regard the results as an estimate for a lower limit of operational stability, or even TTN. We expected a range of $t_{1/2}$ up to 11 h, requiring a starting ketone load of 2 mM. From these reactions on analytical scale, we calculated the residual activity after a certain reaction time by quantification of the remaining substrate by calibrated GC-MS. We also determined a quantitative recovery of the lactone product after appropriate work-up of the reaction.

In the first two sets of conditions we could corroborate our finding that only a large excess of NADPH stabilizes FMO function (Figure 5a). Here, $NADP^+$ and an enzymatic cofactor recycling system was set in place. The sacrificial substrate glucose was supplied in sufficient excess ($\geq 3\ K_M$) to ensure efficient maintenance of the NADPH titer (Figure 5a: pink circles, b: Conditions a).[36]

Increasing the stabilizing power of the formulation (addition of FAD, ROS enzymes, and more NADPH) led to a strong improvement of $t_{1/2}$ under turnover conditions. We observed a much higher stabilizing effect of FAD and NADPH without CAT and SOD in this assay form than in the incubation experiments (322 min *vs.* 99 min, Figure 5b, Conditions b *vs.* Figure 4a, Conditions e). This difference likely arose from the constantly high supply of NADPH provided by the recycling system, and reduction of uncoupling by the synthetic reaction; both were only possible under turnover conditions. With the two best combinations of additives we achieved a quantitative translation of the gain in $t_{1/2}$ from incubation to turnover conditions (approx. 9–12 h, *cf.* Figure 4a, Conditions l *vs.* Figure 5b, Conditions c and d).

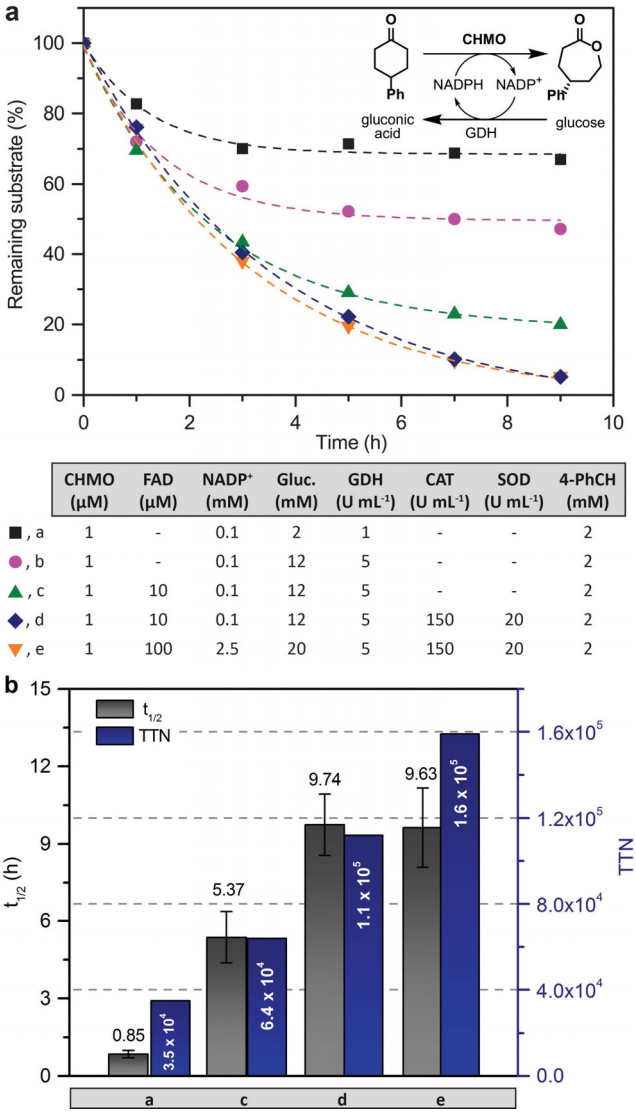

	CHMO (μM)	FAD (μM)	NADP+ (mM)	Gluc. (mM)	GDH (U mL^{-1})	CAT (U mL^{-1})	SOD (U mL^{-1})	4-PhCH (mM)
■, a	1	-	0.1	2	1	-	-	2
●, b	1	-	0.1	12	5	-	-	2
▲, c	1	10	0.1	12	5	-	-	2
◆, d	1	10	0.1	12	5	150	20	2
▼, e	1	100	2.5	20	5	150	20	2

Figure 5. The positive effect of stabilizing additives is quantitatively retained under turnover conditions. (a) Oxidation of 4-phenylcyclohexanone (4-PhCH) to the corresponding (−)-lactone using CHMO at various degrees of stabilization. Cofactor regeneration was performed by supplying glucose (gluc), glucose dehydrogenase (GDH) and $NADP^+$. Reaction progress was monitored via quantification of remaining substrate in EtOAc extracts by calibrated GC-MS. (b) $t_{1/2}$ and estimated TTN values were obtained from exponential fit of catalytic enzyme activity under turnover conditions. Deactivation rate constants are shown in the Supporting Information, Table S9 and kinetic curves are depicted in Figure S15. Data are reported as mean ±1 SD (n = 3).

Conclusions

Our results established a potent protocol for the stabilization of three unrelated class B FMOs, strongly indicating the potential for general application in this class of enzymes. Additionally, these results explain the massive variation of published stability data for CHMO and largely remove this discrepancy by careful control and validation of assay parameters. Surpassing that, we demonstrated with high reproducibility the capability to stabilize a notoriously fragile biocatalyst to more than two days of $t_{1/2}$ through a combination of biogenic additives at room temperature. The choice of optimum reaction parameters (enzyme con-

centration, additives, temperature) resulted in relative improvement of stability by more than three orders of magnitude. Quantitative translation of the enzyme's lifetime to turnover conditions was shown with indicative examples of conditions, using a prochiral substrate to emphasize the enzyme's strength in asymmetric catalysis.

We based our hypotheses on the principle of functional stabilization of CHMO and thus investigated: (i) the role of both cofactors, NADPH and FAD, for structural stability and the denaturation of the catalyst, and (ii) the detrimental influence of ROS, whose generation is difficult to circumvent in this enzyme class. We found that application of Le Chatelier's principle to the non-covalently bound cofactors is by far more effective than any other previously known stabilization attempt for CHMO (with the exception of a heavily mutated industrial variant). Notwithstanding, our concept was demonstrated to be independent of amino acid sequence.

Interestingly, the only reported estimate for the K_d of CHMO-FAD ($K_d = 40$ nM)[8a] established the notion of tight binding in CHMO (and general BVMO/class B FMO) literature, now prevalent for almost 40 years.[37] We found a much higher value than expected, by performing reconstitution experiments of apo-CHMO with FAD, with two independent methods. The newly estimated K_d (approx. 4 μM) explained the unfavorable equilibrium of FAD-FMO binding. The high K_d for FAD also points out a promising strategy for protein engineering in this enzyme class.

Experiments with NADPH revealed that both its total amount of substance as well as its concentration influences the stability of CHMO. The first effect became apparent in our incubation studies, where it was impractical to suppress FMOs' futile activity of oxidizing NADPH with oxygen. As soon as the electron/hydride source was depleted, its structural support feature was concomitantly lost, and the biocatalyst decayed at a much higher rate. When we supplied a larger amount of NADPH in multiple portions, the lifetime could be extended almost linearly; with a high starting amount (and thus higher concentration), the effect was, then inexplicably, significantly larger. Analysis of the thermodynamic stability *via* DSF clearly corroborated this finding, showing a surprisingly steep jump in the melting temperature of CHMO at approx. 1 mM NADPH. It is evident that two independent modes of stabilization can be effected by excess supply of NADPH.

We successfully mitigated the effects of ROS, inevitably produced in FMO reactions, by employing the commercially available and redox-neutral enzymes CAT and SOD in our additive mix. The importance of this second main aspect in our aim for functional stabilization only became apparent with the accumulation of ROS at longer $t_{1/2}$, or with slow substrates (competition between activities). These results indicated that a considerable portion of peroxy inter mediate uncoupled *via* the superoxide pathway. This route generates two equivalents of ROS from one molecule of O_2, compared to only one equivalent of H_2O_2.[26] Superoxide is thus a bigger detrimental factor than H_2O_2 in FMO catalysis. We argue that only a combination of SOD and CAT can be entirely beneficial to stability in oxygen-activating biocatalysis.

The translation from incubation to turnover conditions has previously been described as troublesome in general,[38] and also explicitly for CHMO.[17] We were able to quantitatively translate the achieved stabilization under true reaction conditions (the synthetic reaction lasted for more than one period of $t_{1/2}$), and with a prochiral substrate. Conclusively, this work presents the most effective method for generic FMO stabilization to date. Our rational approach enabled unaltered application of the protocol to two other enzymes of the class, rendering it promising as a sequence-independent, and thus time-efficient method for the stabilization of class B FMOs, and likely other flavin-dependent enzymes.

Experimental Section

Materials

All chemicals and the enzymes superoxide dismutase (SOD, recombinantly expressed in *Escherichia coli*), catalase (CAT) from bovine liver, and glucose oxidase and catalase from *Aspergillus niger* were obtained from Sigma Aldrich and used without further purification unless otherwise stated. NAD^+/$NADP^+$-dependent glucose dehydrogenase (GDH) from *Bacillus* sp. was a kind gift from Amano Enzyme Inc. (Nagoya, Japan).

Growth of Bacterial Cells for Enzyme Expression and Isolation

CHMO (cyclohexanone monooxygenase from *Acinetobacter calcoaceticus* NCIMB 9871) and OTEMO (2-oxo-Δ^3-4,5,5-trimethylcyclopenthenylacetyl-CoA monooxygenase) were expressed in *E. coli* strain BL21(DE3). Lysogeny broth (LB) medium (10 mL) supplemented with ampicillin (100 μg mL^{-1}) or kanamycin (50 μg mL^{-1}) was inoculated with either *E.coli* BL21(DE3) pET22b(+)_CHMO[39] or *E.coli* BL21(DE3) pET28_OTEMO,[40] respectively. These were grown over-night at 37 °C in an orbital shaker operated at 200 rpm. The cultures were transferred to a 2-L Erlenmeyer flask containing 500 mL of a LB/ampicillin or LB/kanamycin medium, which was shaken at 200 rpm and 37 °C for approximately 2.5 h to a final optical cell density at 590 nm of 0.6–0.8. Isopropyl β-D-thiogalactopyranoside (IPTG) was added to a concentration of 50 μM (CHMO) or 10 μM (OTEMO) and flasks were incubated for 18–22 h at 20 °C and 22 °C, respectively. Cells were harvested by centri-

fugation (4000×*g*, 15 min). FMO-E (flavin-containing monooxygenase from *Rhodococcus jostii* RHA1) was obtained in *E.coli* TOP10 pBAD NS FMO-E as previously described by Riebel et al. (2014).[34]

Enzyme Purification

Cell pellets were re-suspended in 50 mM Tris-HCl buffer, pH 8.0, containing phenylmethylsulfonyl fluoride (PMSF, 0.1 mM) and FAD (0.1 mM). Cells were placed on ice and sonicated using a Bandelin KE76 sonotrode connected to a Bandelin Sonoplus HD 3200 in 9 cycles (5 s pulse, 55 s break, amplitude 50%). Precipitates were removed by centrifugation (45 min, 15000×*g*) and the clear supernatants containing the polyhistidine-tagged CHMO and OTEMO wild-type enzymes were loaded on a Ni^{2+}-Sepharose HP affinity column (5 mL, GE Healthcare bioscience) equilibrated with 50 mM Tris-HCl buffer, pH 8.0, containing 0.5 M NaCl. Enzymes were eluted in 4 column volumes within a linear gradient from 25 to 250 mM imidazole in 50 mM Tris-HCl buffer, pH 8.0, containing 0.5 M NaCl. Fractions containing the enzymes were identified by SDS-PAGE analysis, pooled, desalted, washed with 50 mM Tris-HCl, pH 8.5, and concentrated by ultrafiltration by using ultracentrifugal tubes with a cut-off of 10 kDa. FMO was purified employing a Strep-Tactin® Sepharose resin (IBA GmbH, Germany) by following the recommendations of the manufacturer and the minor modifications reported by Riebel et al. (2014).[34] Protein concentrations were determined by the dye-binding method of Bradford using a pre-fabricated assay (Bio-Rad) and bovine serum albumin as the calibration standard.

Steady-State Kinetics

Enzyme activities were measured by monitoring the substrate-dependent decrease in NADPH absorbance at 340 nm ($\varepsilon_{340}=6.22\ mM^{-1}cm^{-1}$). Standard assays contained CHMO (0.05 μM), NADPH (100 μM) and cyclohexanone (0.5 mM) for CHMO or *rac*-bicyclo[3.2.0]hept-2-en-6-one (0.5 mM) for OTEMO and FMO-E in 50 mM Tris-HCl, pH 8.5. The enzyme volume necessary for a final enzyme concentration of 0.05 μM was taken from an incubated solution (enzyme with or without additives) and added to a pre-warmed reaction mix (30 °C) containing the substrate. The reaction was started immediately after enzyme addition by mixing 4 μL NADPH (25 mM stock solution) to the cuvette (final volume 1 mL). Oxidation of NADPH was followed for 120 s at 30 °C in a Lambda 35 spectrophotometer (Perkin–Elmer, Waltham, MA, USA) featuring a thermo-controlled 8-cell changer. All kinetic measurements were performed in triplicate unless otherwise stated. For the determination of the catalytic constants (K_M and k_{cat}), reactions were started by mixing the enzyme solution (final concentration = 0.05 μM) with pre-warmed solutions (25 °C) containing cyclohexanone (0.5 mM) and variable concentrations of NADPH (1.5–200 μM) and variable concentrations of cyclohexanone (1.0–200 μM). Enzyme activity is defined as the amount of enzyme that oxidizes 1 μmol NADPH per minute under the specified conditions. Specific activities were calculated from the observed rate constants (k_{obs}), which were obtained by fitting the initial rate of the absorbance changes to a linear regression (UV WinLab, Perkin–Elmer). Catalytic constants were determined by fitting the observed data to the Michaelis–Menten equation with and without substrate inhibition (SigmaPlot 11 for Windows, Systat Software). Data are reported as $\bar{x}\pm1$ SD (n = 3) unless otherwise stated.

Stopped-Flow Kinetics

Kinetic studies were performed with a SX-20 stopped-flow spectrophotometer (Applied Photophysics, Leatherhead, U.K.) equipped with a SX/PDA photodiode array detector. NADPH (100 μM) and cyclohexanone (0.5 mM) were mixed with CHMO (0.05 μM) in single-mixing mode and the substrate-dependent decrease in NADPH absorbance was recorded at 340 nm ($\varepsilon_{340}=6.22\ mM^{-1}cm^{-1}$). Indicated concentrations are those after mixing. All measurements were performed at 30 °C and at least in triplicate for all investigated conditions. Observed rate constants (k_{obs}) were obtained by fitting the initial rate of the absorbance change to a linear regression using the Pro-Data software suite (Applied Photophysics). Data are reported as $\bar{x}\pm1$ SD (n = 3).

Determination of SOD and CAT Activities

Catalytic activities of SOD, CAT from bovine liver and CAT from *A. niger* were measured in 50 mM Tris-HCl buffer, pH 8.5, at 30 °C following the procedure described by the supplier[41] in triplicate experiments. The supplied enzymes had the following volumetric activities: SOD = 4120 ± 650 U mL^{-1}, CAT = 10000 ± 928 U mL^{-1}. Data are reported as $\bar{x}\pm1$ SD (n = 3).

Determination of the Dissociation Constant (K_d)

FAD-free apoenzymes were generated by column chromatography. Therefore, cleared cell-free extracts were re-suspended in 50 mM Tris-HCl buffer, pH 8.0, containing 0.5 M NaCl and 25 mM imidazole and loaded onto a Ni^{2+}-Sepharose HP resin (5 mL, GE Healthcare) equilibrated with the same buffer. After loading the extract at a flow rate of 0.5 mL min^{-1}, the protein-bound FAD was removed by washing the column with 250 mM phosphate buffer, pH 8.0, containing 3 M KBr. This resulted in a column-bound apoform of the protein, which was eluted with 50 mM Tris-HCl buffer, pH 8.0, containing 0.5 M NaCl and 250 mM imidazole at a flow rate of 5 mL min^{-1}. The apoenzyme was desalted, washed with 50 mM Tris-HCl, pH 8.5, and concentrated by ultrafiltration using ultracentrifugal tubes with a 10 kDa cut-off. Protein concentrations were determined by the dye-binding method of Bradford using a pre-fabricated assay (Bio-Rad) and bovine serum albumin as the calibration standard. The catalytic activities for the determination of the dissociation constants of CHMO and OTEMO were measured after deflavination. For that, 1 μM apoenzyme was incubated with different amounts of FAD (0–200 μM, 5 min incubation at 21 °C) and aliquots were taken for the activity measurement. The specific activity was obtained according to the protocol described above in the paragraph steady-state kinetics and the values plotted *vs.* concentration of FAD. The measurements were performed in triplicate for CHMO and as single experiment for OTEMO due to the high instability of the apoenzyme. The K_d was determined by fitting the data of catalytic activity of the holoenzyme *versus* concentration of FAD with a logistic function (Origin 8.5 for Windows). Data are reported as

$\bar{x} \pm 1$ SD (n = 3) for the experiments with CHMO. Alternatively, the K_d was determined by fluorescence quenching according to a published protocol.[30] Experiments were performed on a Cary Eclipse fluorescence spectrophotometer equipped with a temperature-controlled 4-cell holder (all equipment from Agilent Technologies). Assays were performed at 30 °C and had a total volume of 2 mL containing 1 μM of purified FAD in 50 mM Tris-HCl buffer, pH 8.5. Addition of increasing concentrations of apo-CHMO quenched the FAD fluoresecence at 520 nm upon excitation at 350 nm. The weak unspecific fluorescence from apo-CHMO alone was substracted from all data. The K_d was calculated for the data sets obtained for added CHMO concentrations between 0.8 and 5 μM using the correlation: K_d = ([free CHMO] × [free FAD])/CHMO-FAD. Data are reported as $\bar{x} \pm 1$ SD (n = 3).

Stability Measurements

Stability measurements were performed by incubating 0.05–100 μM enzyme at 30 °C (unless stated otherwise) in 50 mM Tris-HCl, pH 8.5, containing variable concentrations of desired additives (0–100 μM FAD; 0.1–2.5 mM NADPH; 400 U mL^{-1} SOD and/or 100 U mL^{-1} CAT). Aliquots were taken at different time points and added to a cuvette containing 100 μM NADPH and 0.5 mM substrate to test for catalytic activity. In the case of stopped-flow measurements, activity was measured automatically at defined time intervals. All kinetics measurements were performed at 30 °C. The experimental data were fitted to an exponential decay equation using the Origin Pro software (Origin 8.5 for Windows). Data are reported as $\bar{x} \pm 1$ SD (n = 3) unless otherwise stated.

Ratio of Activities of ROS Enzymes

We obtained SOD and CAT from commercial vendors and used them without further purification for the experiments under non-turnover conditions. We intended to add a higher equivalent activity of CAT than of SOD to circumvent the build-up of superoxide (approx. ratio 8:1 CAT/SOD), but the trends in stability values were difficult to interpret along our hypothesis. We then post-experimentally determined the specific activity employing the protocols recommended by the supplier, and actually found a reversed ratio of approx. 1:4 CAT/SOD. This was later corrected for the experiments under turnover conditions. Data are reported as $\bar{x} \pm 1$ SD (n = 3).

Transition Midpoint Temperature or Melting Temperature (T_m) Employing NanoDSF

Effect of different concentrations of NADPH (0.1–2.5 mM) on the melting temperature (T_m) of CHMO (15 μM) was evaluated employing a nanoDSF device (Prometheus NT.48, NanoTemper Technologies GmbH). Capillaries were filled directly from respective solutions (10 μL). Samples were measured in the Prometheus NT.48 in a temperature range between 20 °C and 98 °C at various concentrations of NADPH (0.25–2.50 mM, 0.25 mM intervals). Data analysis was performed using NT Melting Control software (NanoTemper Technologies GmbH). The T_m was determined by fitting the tryptophan fluorescence emission ratio of 350 nm to 330 nm using a polynomial function, in which the maximum slope is indicated by the peak of its first derivative. Data are reported as $\bar{x} \pm 1$ SD (n = 3).

Uncoupling Reactions

The uncoupling reaction of the reduced enzyme with O_2 in the presence of NADPH was monitored using an Agilent 8453 UV/Vis spectrophotometer with a photodiode array detector. For these experiments, the decrease in the absorbance at 340 nm ($\varepsilon_{340nm} = 6.22$ mM^{-1} cm^{-1}) was monitored for mixtures containing CHMO (0.05–1 μM) and NADPH (100 μM) with or without the addition of additives (10 μM FAD, 400 U mL^{-1} SOD and/or 100 U mL^{-1} CAT). Anaerobic conditions were achieved by flushing the solutions with N_2 and removing traces of oxygen by adding glucose (10 mM) and glucose oxidase (10 U mL^{-1}) in the presence of CAT (30 U mL^{-1}). The uncoupling rate constants were determined by fitting the curves with a linear regression using the Origin Pro software (Origin 8.5 for Windows). Data are reported as $\bar{x} \pm 1$ SD (n = 3).

Determination of H_2O_2 Formation

Hydrogen peroxide H_2O_2 was measured by a 2,2′-azinobis(3-ethylbenzothiazoline-6-sulfonate) (ABTS)-based assay. This assay quantifies the production of H_2O_2 by oxidases through the oxidation of ABTS in the presence of horseradish peroxidase. The formation of the green ABTS radical cation was followed spectrophotometrically at 420 nm (ε_{420nm} = 36 mM^{-1} cm^{-1}). The colorimetric reaction was started by the addition of 1 μM CHMO to a mixture containing 100 μM NADPH, 2 mM ABTS and 5.8 U mL^{-1} peroxidase in 50 mM Tris-HCl, pH 8.5. The increase in absorbance was followed using an Agilent 8453 UV/Vis spectrophotometer equipped with a photodiode array detector. The effect of SOD on the H_2O_2 formation rate was measured by adding 400 U mL^{-1} SOD to the mixture. Enzyme kinetics were measured at 30 °C in the presence of a fast substrate, cyclohexanone, or a slow substrate, 4-phenylcyclohexanone. The stoichiometry of this reaction is two since one mole of H_2O_2 and two moles of the ABTS cation radical are formed.[42] The formation rate of H_2O_2 was determined by fitting the observed data to a linear equation using the Origin Pro software (Origin 8.5 for Windows). Data are reported as $\bar{x} \pm 1$ SD (n = 3).

Size Exclusion Chromatography

Analytical size exclusion chromatography was performed with a Sephadex 75 column (24 mL; column diameter, 10 mm) using 50 mM Tris-HCl buffer (pH 8.5) at a flow rate of 0.8 mL min^{-1} (all chromatographic equipment from GE Healthcare). The column was calibrated with protein standards (bovine serum albumin; 66 kDa, ovalbumin, 43 kDa, carbonic anhydrase, 29 kDa; ribonuclease A 13.7 kDa; aprotinin, 6.5 kDa) obtained from commercial suppliers.

Acknowledgements

We thank David Siebert (TU Wien) for the purification of FAD, Dr. Anna Münch (NanoTemper Technologies GmbH) for generously providing access to the DSF fluorimeter, and Prof. Marco W. Fraaije (University of Groningen) for kindly providing a sample of the CHMO-PTDH fusion enzyme. This work was supported by the Austrian Science Fund FWF (grants no. I723-N17 and P24483-B20), by the COST action Systems Biocatalysis WG2, by TU Wien (ABC-Top Anschubfinanzierung), by the European Commission Project INDOX (grant no. FP7-KBBE-2013-7-613549), and by the Coordination for the Improvement of Higher Education Personnel (grant no. CAPES/CsF, 2505-13-4).

References

[1] a) M. M. E. Huijbers, S. Montersino, A. H. Westphal, D. Tischler, W. J. H. van Berkel, *Arch. Biochem. Biophys.* **2014**, *544*, 2–17; b) N. L. Schlaich, *Trends Plant Sci.* **2007**, *12*, 412–418; c) P. Chaiyen, M. W. Fraaije, A. Mattevi, *Trends Biochem. Sci.* **2012**, *37*, 373–380.

[2] a) S. K. Krueger, D. E. Williams, *Pharmacol. Ther.* **2005**, *106*, 357–387; b) S. F. Leiser, H. Miller, R. Rossner, M. Fletcher, A. Leonard, M. Primitivo, N. Rintala, F. J. Ramos, D. L. Miller, M. Kaeberlein, *Science* **2015**, *350*, 1375–1378.

[3] W. J. H. van Berkel, N. M. Kamerbeek, M. W. Fraaije, *J. Biotechnol.* **2006**, *124*, 670–689.

[4] a) S. Visitsatthawong, P. Chenprakhon, P. Chaiyen, P. Surawatanawong, *J. Am. Chem. Soc.* **2015**, *137*, 9363–9374; b) T. Wongnate, P. Surawatanawong, S. Visitsatthawong, J. Sucharitakul, N. S. Scrutton, P. Chaiyen, *J. Am. Chem. Soc.* **2014**, *136*, 241–253.

[5] a) I. A. Mirza, B. J. Yachnin, S. Wang, S. Grosse, H. Bergeron, A. Imura, H. Iwaki, Y. Hasegawa, P. C. K. Lau, A. M. Berghuis, *J. Am. Chem. Soc.* **2009**, *131*, 8848–8854; b) B. J. Yachnin, T. Sprules, M. B. McEvoy, P. C. K. Lau, A. M. Berghuis, *J. Am. Chem. Soc.* **2012**, *134*, 7788–7795; c) B. J. Yachnin, M. B. McEvoy, R. J. D. MacCuish, K. L. Morley, P. C. K. Lau, A. M. Berghuis, *ACS Chem. Biol.* **2014**, *9*, 2843–2851.

[6] R. Tinikul, W. Pitsawong, J. Sucharitakul, S. Nijvipakul, D. P. Ballou, P. Chaiyen, *Biochemistry* **2013**, *52*, 6834–6843.

[7] a) A. Mattevi, *Trends Biochem. Sci.* **2006**, *31*, 276–283; b) M. H. Hefti, J. Vervoort, W. J. H. van Berkel, *Eur. J. Biochem.* **2003**, *270*, 4227–4242.

[8] a) N. A. Donoghue, D. B. Norris, P. W. Trudgill, *Eur. J. Biochem.* **1976**, *63*, 175–192; b) J. D. Stewart, *Curr. Org. Chem.* **1998**, *2*, 195–216.

[9] Y. K. Bong, M. D. Clay, S. J. Collier, B. Mijts, M. Vogel, X. Zhang, J. Zhu, J. Nazor, D. Smith, S. Song, WO Patent WO2011071982A2, Codexis Inc., USA, **2011**, 109 pp.

[10] a) H. Leisch, K. Morley, P. C. K. Lau, *Chem. Rev.* **2011**, *111*, 4165–4222; b) K. Balke, M. Kadow, H. Mallin, S. Sass, U. T. Bornscheuer, *Org. Biomol. Chem.* **2012**, *10*, 6249–6265.

[11] F. Rudroff, J. Rydz, F. H. Ogink, M. Fink, M. D. Mihovilovic, *Adv. Synth. Catal.* **2007**, *349*, 1436–1444.

[12] E. Beneventi, G. Ottolina, G. Carrea, W. Panzeri, G. Fronza, P. C. K. Lau, *J. Mol. Catal. B: Enzym.* **2009**, *58*, 164–168.

[13] a) M. J. Fink, F. Rudroff, M. D. Mihovilovic, *Bioorg. Med. Chem. Lett.* **2011**, *21*, 6135–6138; b) M. J. Fink, M. Schoen, F. Rudroff, M. Schnuerch, M. D. Mihovilovic, *ChemCatChem* **2013**, *5*, 724–727.

[14] S. Schmidt, C. Scherkus, J. Muschiol, U. Menyes, T. Winkler, W. Hummel, H. Groeger, A. Liese, H.-G. Herz, U. T. Bornscheuer, *Angew. Chem.* **2015**, *127*, 2825–2828; *Angew. Chem. Int. Ed.* **2015**, *54*, 2784–2787.

[15] a) H. L. van Beek, R. T. Winter, G. R. Eastham, M. W. Fraaije, *Chem. Commun.* **2014**, *50*, 13034–13036; b) M. J. Fink, M. D. Mihovilovic, *Chem. Commun.* **2015**, *51*, 2874–2877.

[16] F. Secundo, F. Zambianchi, G. Crippa, G. Carrea, G. Tedeschi, *J. Mol. Catal. B: Enzym.* **2005**, *34*, 1–6.

[17] F. Zambianchi, P. Pasta, G. Carrea, S. Colonna, N. Gaggero, J. M. Woodley, *Biotechnol. Bioeng.* **2002**, *78*, 489–496.

[18] S. Staudt, U. T. Bornscheuer, U. Menyes, W. Hummel, H. Groeger, *Enzyme Microb. Technol.* **2013**, *53*, 288–292.

[19] H. L. van Beek, H. J. Wijma, L. Fromont, D. B. Janssen, M. W. Fraaije, *FEBS Open Bio* **2014**, *4*, 168–174.

[20] S. Schmidt, M. Genz, K. Balke, U. T. Bornscheuer, *J. Biotechnol.* **2015**, *214*, 199–211.

[21] a) H. L. van Beek, G. de Gonzalo, M. W. Fraaije, *Chem. Commun.* **2012**, *48*, 3288–3290; b) D. J. Opperman, M. T. Reetz, *ChemBioChem* **2010**, *11*, 2589–2596.

[22] R. H. H. van den Heuvel, N. Tahallah, N. M. Kamerbeek, M. W. Fraaije, W. J. H. van Berkel, D. B. Janssen, A. J. R. Heck, *J. Biol. Chem.* **2005**, *280*, 32115–32121.

[23] E. Romero, J. R. G. Castellanos, A. Mattevi, M. W. Fraaije, *Angew. Chem.* **2016**, *128*, 16084–16087; *Angew. Chem. Int. Ed.* **2016**, *128*, 15852–15855.

[24] T. A. Rogers, A. S. Bommarius, *Chem. Eng. Sci.* **2010**, *65*, 2118–2124.

[25] A. S. Bommarius, M. F. Paye, *Chem. Soc. Rev.* **2013**, *42*, 6534–6565.

[26] J. A. Imlay, *Nature Rev. Microbiol.* **2013**, *11*, 443–454.

[27] A. Beier, S. Bordewick, M. Genz, S. Schmidt, T. van den Bergh, C. Peters, H.-J. Joosten, U. T. Bornscheuer, *ChemBioChem* **2016**, *17*, 2312–2315.

[28] a) D. Sheng, D. P. Ballou, V. Massey, *Biochemistry* **2001**, *40*, 11156–11167; b) N. M. Kamerbeek, M. W. Fraaije, D. B. Janssen, *Eur. J. Biochem.* **2004**, *271*, 2107–2116.

[29] At these elevated temperatures a new mechanism of deactivation became apparent, showing an induction period (15 min) before the exponential decay. We therefore used the average lifetime for quantitative comparison.

[30] a) J. Becvar, G. Palmer, *J. Biol. Chem.* **1982**, *257*, 5607–5617; b) L. J. Druhan, R. P. Swenson, *Biochemistry* **1998**, *37*, 9668–9678; c) M. J. Hamill, M. Jost, C. Wong, S. J. Elliott, C. L. Drennan, *Biochemistry* **2011**, *50*, 10159–10169.

[31] F. Müller, W. J. H. van Berkel, *Eur. J. Biochem.* **1982**, *128*, 21–27.

[32] M. H. Hefti, F. J. Milder, S. Boeren, J. Vervoort, W. J. H. van Berkel, *Biochim. Biophys. Acta Gen. Subj.* **2003**, *1619*, 139–143.
[33] a) M. Kadow, K. Loschinski, S. Sass, M. Schmidt, U. T. Bornscheuer, *Appl. Microbiol. Biotechnol.* **2012**, *96*, 419–429; b) H. Leisch, R. Shi, S. Grosse, K. Morley, H. Bergeron, M. Cygler, H. Iwaki, Y. Hasegawa, P. C. K. Lau, *Appl. Environ. Microbiol.* **2012**, *78*, 2200–2212.
[34] A. Riebel, M. J. Fink, M. D. Mihovilovic, M. W. Fraaije, *ChemCatChem* **2014**, *6*, 1112–1117.
[35] D. V. Rial, D. A. Bianchi, P. Kapitanova, A. Lengar, J. B. van Beilen, M. D. Mihovilovic, *Eur. J. Org. Chem.* **2008**, *2008*, 1203–1213.
[36] V. Kaswurm, W. Van Hecke, K. D. Kulbe, R. Ludwig, *Adv. Synth. Catal.* **2013**, *355*, 1709–1714.
[37] a) C. C. Ryerson, D. P. Ballou, C. Walsh, *Biochemistry* **1982**, *21*, 2644–2655; b) C. T. Walsh, Y. C. J. Chen, *Angew. Chem.* **1988**, *100*, 342–352; *Angew. Chem. Int. Ed. Engl.* **1988**, *27*, 333–343; c) M. Krzek, H. L. van Beek, H. P. Permentier, R. Bischoff, M. W. Fraaije, *Enzyme Microb. Technol.* **2016**, *82*, 138–143.
[38] V. Stepankova, S. Bidmanova, T. Koudelakova, Z. Prokop, R. Chaloupkova, J. Damborsky, *ACS Catal.* **2013**, *3*, 2823–2836.
[39] G. Chen, M. M. Kayser, M. D. Mihovilovic, M. E. Mrstik, C. A. Martinez, J. D. Stewart, *New J Chem.* **1999**, *23*, 827–832.
[40] M. Kadow, K. Loschinski, S. Sass, M. Schmidt, U. T. Bornscheuer, *Appl Microbiol Biot* **2012**, *96*, 419–429.
[41] a) R. F. Beers Jr, I. W. Sizer, *J. Biol. Chem.* **1952**, *195*, 133–140; b) K. G. Stern, *J. Biol. Chem.* **1937**, *121*, 561–572; c) J. M. McCord, I. Fridovich, *J. Biol. Chem.* **1969**, *244*, 6049–6055.
[42] C. Sygmund, P. Santner, I. Krondorfer, C. K. Peterbauer, M. Alcalde, G. S. Nyanhongo, G. M. Guebitz, R. Ludwig, *Microb. Cell Fact.* **2013**, *12*, 38.

